

CONVERGENT NUMERICAL METHOD FOR A LINEARIZED TRAVEL TIME TOMOGRAPHY PROBLEM WITH INCOMPLETE DATA *

MICHAEL V. KLIBANOV[†], THUY T. LE[†], AND LOC H. NGUYEN[†]

Abstract. We propose a new numerical method to solve the linearized problem of travel time tomography with incomplete data. Our method is based on the technique of the truncation of the Fourier series with respect to a special basis of L^2 . This way we derive a boundary value problem for a system of coupled partial differential equations (PDEs) of the first order. This system is solved by the quasi-reversibility method. Hence, the spatially dependent Fourier coefficients of the solution to the linearized Eikonal equation are obtained. The convergence of this method is established. Numerical results for highly noisy data are presented.

Key words. linearization, inverse kinematic problem, travel time tomography, numerical solution, convergence

AMS subject classifications. 35R25, 35R30

1. Introduction. In this paper we develop a new numerical method for the linearized Travel Time Tomography Problem (TTTP) for the d -D case. Our data are both non-redundant and incomplete. Using a discrete Carleman estimate, we establish the convergence of our method. In addition, we provide results of numerical experiments in the 2D case. In particular, we demonstrate that our method provides good accuracy of images of complicated objects with 5% noise in the data. Furthermore, a satisfactory accuracy of images is demonstrated even for very high levels of noise between 30% and 120%.

In fact, both the idea of our method and sources/detectors configuration are close to those of our recent works [15, 31]. However, our case is substantially more difficult one since the waves in our case propagate along geodesic lines, rather than a radiation propagating along straight lines in [15, 31]. Still, although we formulate here results related to the convergence of our method, we do not prove them. The reason is that, as it turns out, proofs are very similar to those in [31]. In other words, surprisingly, the analytical apparatus of the convergence theory developed in [31] works well for the problem considered in this paper.

In the isotropic case of acoustic/seismic waves propagation, the travel time tomography problem (TTTP) is the problem of the recovery of the spatially distributed speed of propagation of acoustic/seismic waves from the first times of arrival of those waves. In the electromagnetic case this is the problem of the recovery of the spatially distributed dielectric constant from those times. Another name for the TTTP is inverse kinematic problem (IKP). Waves are originated by some sources located either at the boundary of the closed bounded domain of interest or outside of this domain. Times of first arrival from those sources are measured on a part of the boundary of that domain. The TTTP has well known applications in Geophysics, see, e.g. the book of Romanov [27, Chapter 3].

The history of the TTTP has started 114 years ago. The pioneering papers about the solution of the 1D TTTP were published by Herglotz [5] (1905) and then

* **Funding.** The work was supported by US Army Research Laboratory and US Army Research Office grant W911NF-19-1-0044.

[†]Department of Mathematics and Statistics, University of North Carolina at Charlotte, Charlotte, NC 28223, USA, mklibanv@uncc.edu (corresponding author), tle55@uncc.edu, loc.nguyen@uncc.edu

by Wiechert and Zoeppritz [35] (1907). Their method is described in the book of Romanov [27, Section 3 of Chapter 3]. It was discovered recently that, in addition to Geophysics, the IKP has applications in the phaseless inverse scattering problem [16, 17, 28].

The next natural question after the classical 1D case of [5, 35] was about 2 and 3 dimensional cases. The first uniqueness and Lipschitz stability result for the 2D case was obtained by Mukhometov [22], also see [1, 25]. Next, these results were obtained by Mukhometov and Romanov for the 3D case in [23, 27]. We also refer to the work of Stefanov, Uhlmann and Vasy [32] for a more recent publication for the 3D case. As to the numerical methods for the inverse kinematic problem, we refer to [29] for the 2D case and to [36] for the 3D case.

In all past publication about the IKP, the data are redundant in the 3D case and complete in both 2D and 3D cases. In two recent works of the first author [12, 13] two globally convergent numerical methods for the 3D TTTP with non redundant incomplete data were developed.

Along with the full IKP, a significant applied interest is also in a linearized IKP, see [27, Chapter 3]. Let c be the speed of sound. Denote $\mathbf{n} = 1/c$ the refractive index. To linearize, one should assume that $\mathbf{n} = \mathbf{n}_0 + \mathbf{n}_1$, where \mathbf{n}_0 is the known background function and \mathbf{n}_1 with $|\mathbf{n}_1| \ll \mathbf{n}_0$ is its unknown perturbation, which is the subject to the solution of the linearized TTTP. Thus, one assumes that the refractive index is basically known, whereas its small perturbation \mathbf{n}_1 is unknown. This problem is also called the *geodesic X-ray transform problem*. The Lipschitz stability and uniqueness theorem for this problem in the isotropic case was first obtained in [26], see Theorem 3.2 in Section 4 of Chapter 3 of [27]. In the non isotropic case this problem was studied in [33]. In [21] numerical studies of this problem in the isotropic case were performed.

In our derivation, we end up with an over determined boundary value problem for a system of coupled linear PDEs of the first order. It is well known that the quasi-reversibility method is an effective tool for numerical solutions of over determined boundary value problems for PDEs. Lattès and Lions [18] were the first ones who have proposed the quasi-reversibility method. This technique was developed further in, e.g. [2, 3, 6, 10, 15, 20, 31]. In particular, it was shown in [10] that while it is rather easy to prove, using Riesz theorem, the existence and uniqueness of the minimizer of a certain functional related to this method, the proof of convergence of those minimizers to the correct solution requires a stronger tool of Carleman estimates.

Another important feature of this paper is a special orthonormal basis in the space $L^2(-\bar{\alpha}, \bar{\alpha})$, where $\bar{\alpha} > 0$ is a certain number. The functions of this basis depend only on the position of the point source. This basis was first introduced in [11] and was further used in [12, 13, 15, 31]. Just like in our previous publications [12, 13, 15, 31], we use here an *approximate mathematical model*. More precisely, we assume that a certain function associated with the solution of the governing linearized Eikonal equation can be represented via a truncated Fourier series with respect to this basis. This assumption forms the first element of that model. The second element is that we assume that the first derivatives with respect to all variables, except of one, are written via finite differences and the step size of these finite differences is bounded from the below by a positive number $h_0 > 0$.

We do not prove convergence as the number N of terms in that truncated series tends to infinity and the lower bound for the grid step h_0 size tends to zero. Thus, we come up with a semi-finite dimensional approximate mathematical model. We point out that similar approximate mathematical models are used quite often in studies of

numerical methods for inverse problems by other authors, and numerical results are usually encouraging, see, e.g. [4, 7, 9, 8]. Just as ourselves, proofs of convergence results in such cases when, e.g. $N \rightarrow \infty, h_0 \rightarrow 0$ are usually not conducted since they are very challenging tasks due to the ill-posed nature of inverse problems.

The paper is organized as follows. In Section 2, we formulate the inverse problem. Next, in Section 3, we introduce the truncation technique and our numerical method. Then, in Section 4, we recall the quasi-reversibility method and its convergence in the case of partial finite differences. In Section 5 we present the implementation and numerical results. Finally, Section 6 is for concluding remarks.

2. The linearization. Let $d \geq 2$ be the spatial dimension. Let $R > 1$ and $0 < a < b$. Set

$$(2.1) \quad \Omega = (-R, R)^{d-1} \times (a, b) \subset \mathbb{R}^d.$$

Let $\mathbf{c}_0(\mathbf{x}) = \mathbf{n}_0^2(\mathbf{x})$, $\mathbf{x} \in \Omega$ where \mathbf{n}_0 is the refractive index of the background. Assume that $\mathbf{c}_0 = \mathbf{n}_0^2 = 1$ on $\mathbb{R}^d \setminus \Omega$. For any two points \mathbf{x}_1 and \mathbf{x}_2 in \mathbb{R}^d , define the geodesic line generated by \mathbf{n}_0 connecting \mathbf{x}_1 and \mathbf{x}_2 as:

$$(2.2) \quad \Gamma(\mathbf{x}_1, \mathbf{x}_2) = \operatorname{argmin} \left\{ \int_{\gamma} \mathbf{n}_0(\boldsymbol{\xi}) d\sigma(\boldsymbol{\xi}) \text{ where } \gamma : [0, 1] \rightarrow \mathbb{R}^d \right. \\ \left. \text{is a smooth map with } \gamma(0) = \mathbf{x}_1, \gamma(1) = \mathbf{x}_2 \right\}.$$

Given the refractive index \mathbf{n}_0 , the geodesic line $\Gamma(\mathbf{x}_1, \mathbf{x}_2)$ is the curve connecting points \mathbf{x}_1 and \mathbf{x}_2 and such that the travel time along $\Gamma(\mathbf{x}_1, \mathbf{x}_2)$ is minimal. The travel time is the integral in (2.2). If $\mathbf{n}_0 \equiv 1$, then $\Gamma(\mathbf{x}_1, \mathbf{x}_2)$ is the line segment connecting these two points.

Introduce the line of sources L_{sc} located on the x_1 -axis as

$$(2.3) \quad L_{sc} = [-\bar{\alpha}, \bar{\alpha}] \times \{(0, 0, \dots, 0)\},$$

where $\bar{\alpha}$ is a fixed positive number. For each source position $\mathbf{x}_\alpha = (\alpha, 0, \dots, 0) \in L_{sc}$, the function

$$(2.4) \quad u_0(\mathbf{x}, \mathbf{x}_\alpha) = \int_{\Gamma(\mathbf{x}, \mathbf{x}_\alpha)} \mathbf{n}_0(\boldsymbol{\xi}) d\sigma(\boldsymbol{\xi}) \quad \mathbf{x} \in \mathbb{R}^d$$

is the travel time of the wave from \mathbf{x}_α to \mathbf{x} .

ASSUMPTION 2.1 (regularity of geodesic lines). *We assume everywhere in this paper that the geodesic lines are regular in the following sense: for each point \mathbf{x} of the closed domain $\bar{\Omega}$ and for each point \mathbf{x}_α of the line of sources L_{sc} there exists a single geodesic line $\Gamma(\mathbf{x}, \mathbf{x}_\alpha)$ connecting them.*

For each $\alpha \in (-\bar{\alpha}, \bar{\alpha})$, define

$$\partial\Omega_\alpha^- = \{\mathbf{x} \in \partial\Omega : \nabla u_0(\mathbf{x}, \mathbf{x}_\alpha) \cdot \mathbf{n}(\mathbf{x}) \leq 0\}, \\ \partial\Omega_\alpha^+ = \{\mathbf{x} \in \partial\Omega : \nabla u_0(\mathbf{x}, \mathbf{x}_\alpha) \cdot \mathbf{n}(\mathbf{x}) > 0\}$$

where $\mathbf{x}_\alpha = (\alpha, 0, \dots, 0)$. Let $p : \mathbb{R}^d \rightarrow \mathbb{R}$ be a function compactly supported in Ω . For each $\mathbf{x}_\alpha \in L_{sc}$, let $u(\mathbf{x}, \mathbf{x}_\alpha)$ be the solution to

$$(2.5) \quad \begin{cases} \nabla u_0(\mathbf{x}, \mathbf{x}_\alpha) \cdot \nabla u(\mathbf{x}, \mathbf{x}_\alpha) = p(\mathbf{x}), & \mathbf{x} \in \Omega, \\ u(\mathbf{x}, \mathbf{x}_\alpha) = 0, & \mathbf{x} \in \Omega^-. \end{cases}$$

The aim of this paper is to solve the following inverse problem:

PROBLEM 2.1 (linearized travel time tomography problem). *Given the data*

$$(2.6) \quad f(\mathbf{x}, \mathbf{x}_\alpha) = u(\mathbf{x}, \mathbf{x}_\alpha), \quad \mathbf{x} \in \partial\Omega^+, \mathbf{x}_\alpha \in L_{sc},$$

determine the function $p(\mathbf{x})$, $\mathbf{x} \in \Omega$.

Remark 2.1. The data $f(\mathbf{x}, \mathbf{x}_\alpha)$ are non-redundant ones. Indeed, the source $\mathbf{x}_\alpha \in L_{sc}$ depends on one variable and $\mathbf{x} \in \partial\Omega^+$ depends on $d - 1$ variables. Hence the function $f(\mathbf{x}, \mathbf{x}_\alpha)$ depends on d variables, so does the target function $p(\mathbf{x})$.

Problem 2.1 arises from the highly nonlinear and severely ill-posed inverse kinematic problem. Assume that $\mathbf{c}(\mathbf{x}) = \mathbf{n}^2(\mathbf{x})$ contains a perturbation term of the background function $\mathbf{c}_0(\mathbf{x}) = \mathbf{n}_0^2(\mathbf{x})$. In other words,

$$(2.7) \quad \mathbf{c}(\mathbf{x}) = \mathbf{c}_0(\mathbf{x}) + 2\epsilon p(\mathbf{x}) \quad \mathbf{x} \in \mathbb{R}^d$$

for a small number $\epsilon > 0$. Denote by

$$u_{\mathbf{n}}(\mathbf{x}, \mathbf{x}_\alpha) = \int_{\Gamma_{\mathbf{n}}(\mathbf{x}, \mathbf{x}_\alpha)} \mathbf{n}(\xi) d\sigma(\xi)$$

the travel time from $\mathbf{x}_\alpha \in L_{sc}$ to $\mathbf{x} \in \Omega$, where $\Gamma_{\mathbf{n}}(\mathbf{x}, \mathbf{x}_\alpha)$ is the geodesic line generated by the function \mathbf{n} . Then, it is well-known [27] that $u(\mathbf{x}, \mathbf{x}_\alpha)$ satisfies the Eikonal equation

$$(2.8) \quad |\nabla u_{\mathbf{n}}(\mathbf{x}, \mathbf{x}_\alpha)|^2 = \mathbf{c}(\mathbf{x}) \quad \mathbf{x} \in \Omega, \mathbf{x}_\alpha \in L_{sc}.$$

The inverse kinematic problem is to determine the function \mathbf{c} from the measurement of $u(\mathbf{x}, \mathbf{x}_\alpha)$ for all $\mathbf{x} \in \partial\Omega^+$ and $\mathbf{x}_\alpha \in L_{sc}$. Let $u_0(\mathbf{x}, \mathbf{x}_\alpha)$ be the travel time function corresponding to the background \mathbf{c}_0 . Then, one has

$$(2.9) \quad |\nabla u_0(\mathbf{x}, \mathbf{x}_\alpha)|^2 = \mathbf{c}_0(\mathbf{x}) \quad \mathbf{x} \in \Omega, \mathbf{x}_\alpha \in L_{sc}.$$

Due to (2.7) we represent $\nabla u_{\mathbf{n}}(\mathbf{x}, \mathbf{x}_\alpha)$ as $\nabla u_{\mathbf{n}}(\mathbf{x}, \mathbf{x}_\alpha) = \nabla u_0(\mathbf{x}, \mathbf{x}_\alpha) + \epsilon \nabla u^{(1)}(\mathbf{x}, \mathbf{x}_\alpha)$. Hence, ignoring the term with ϵ^2 , we obtain

$$|\nabla u_{\mathbf{n}}(\mathbf{x}, \mathbf{x}_\alpha)|^2 \approx |\nabla u_0(\mathbf{x}, \mathbf{x}_\alpha)|^2 + 2\epsilon \nabla u_0(\mathbf{x}, \mathbf{x}_\alpha) \nabla u^{(1)}(\mathbf{x}, \mathbf{x}_\alpha).$$

Denoting $u^{(1)} := u$, we obtain

$$\nabla u_0(\mathbf{x}, \mathbf{x}_\alpha) \cdot \nabla u(\mathbf{x}, \mathbf{x}_\alpha) = p(\mathbf{x}).$$

Thus, the inverse source problem under consideration is the ‘‘linearization’’ of the nonlinear kinematic inverse problem.

Note that since the function p is compactly supported in Ω , then $\mathbf{c} = \mathbf{c}_0 = 1$ in $\mathbb{R}^d \setminus \Omega$. This implies that $u_{\mathbf{n}}(\mathbf{x}, \mathbf{x}_\alpha) = u_0(\mathbf{x}, \mathbf{x}_\alpha) = |\mathbf{x} - \mathbf{x}_\alpha|$, for all $\mathbf{x} \in \partial\Omega_\alpha^-$. Hence, we set $u(\mathbf{x}, \mathbf{x}_\alpha) = 0$ for all $\mathbf{x} \in \partial\Omega_\alpha^-$.

From now on, to separate the coordinate number d of the point \mathbf{x} , we write $\mathbf{x} = (x_1, \dots, x_{d-1}, z)$. The transport equation in (2.5) is read as

$$(2.10) \quad \partial_z u_0(\mathbf{x}, \mathbf{x}_\alpha) \partial_z u(\mathbf{x}, \mathbf{x}_\alpha) + \sum_{i=1}^{d-1} \partial_{x_i} u_0(\mathbf{x}, \mathbf{x}_\alpha) \partial_{x_i} u(\mathbf{x}, \mathbf{x}_\alpha) = p(\mathbf{x})$$

for all $\mathbf{x} \in \Omega$, $\mathbf{x}_\alpha \in L_{sc}$.

3. A boundary value problem for a system of coupled PDEs of the first order. This section aims to derive a system of partial differential equations, which can be stably solved by the quasi-reversibility method in the semi-finite difference scheme. The solution of this system yields the desired numerical solution to Problem 2.1.

We will employ a special basis of $L^2(-\bar{\alpha}, \bar{\alpha})$ where $2\bar{\alpha}$ is the length of the line of source L_{sc} , see (2.3). For each $n = 1, 2, \dots$, let $\phi_n(\alpha) = \alpha^{n-1} \exp(\alpha)$. The set $\{\phi_n\}_{n=1}^{\infty}$ is complete in $L^2(-\bar{\alpha}, \bar{\alpha})$. Applying the Gram-Schmidt orthonormalization process to this set, we obtain a basis of $L^2(-\bar{\alpha}, \bar{\alpha})$, named as $\{\Psi_n\}_{n=1}^{\infty}$. We have the proposition

PROPOSITION 3.1 (see [11]). *The basis $\{\Psi_n\}_{n=1}^{\infty}$ satisfies the following properties:*

1. Ψ_n is not identically zero for all $n \geq 1$,
2. For all $m, n \geq 1$

$$s_{mn} = \int_{-\bar{\alpha}}^{\bar{\alpha}} \Psi'_n(\alpha) \Psi_m(\alpha) d\alpha = \begin{cases} 1 & \text{if } m = n, \\ 0 & \text{if } n < m. \end{cases}$$

As a result, for all integer $N > 1$, the matrix $S_N = (s_{mn})_{m,n=1}^N$, is invertible.

REMARK 3.1. *The basis $\{\Psi_n\}_{n=1}^{\infty}$ was first introduced in [11]. Then, this basis was successfully used to solve several important inverse problems, including the inverse source problem for Helmholtz equations [24], inverse X-ray tomographic problem in incomplete data [15] and the nonlinear inverse problem of electrical impedance tomography with the so-called restricted Dirichlet-to-Neumann map data, see [14], the inverse problem of computing the initial condition of nonlinear parabolic equations [19].*

We now derive an important system for Fourier coefficients of the function

$$(3.1) \quad w(\mathbf{x}, \mathbf{x}_\alpha) = u(\mathbf{x}, \mathbf{x}_\alpha) \partial_z u_0(\mathbf{x}, \mathbf{x}_\alpha) \quad \mathbf{x} \in \Omega, \mathbf{x}_\alpha \in L_{sc}$$

with respect to the basis in Proposition 3.1. Differentiate (2.10) with respect to α . We obtain

$$(3.2) \quad \frac{\partial}{\partial \alpha} \left[\partial_z u_0(\mathbf{x}, \mathbf{x}_\alpha) \partial_z u(\mathbf{x}, \mathbf{x}_\alpha) + \sum_{i=1}^{d-1} \partial_{x_i} u_0(\mathbf{x}, \mathbf{x}_\alpha) \partial_{x_i} u(\mathbf{x}, \mathbf{x}_\alpha) \right] = 0$$

for all $\mathbf{x} \in \Omega, \mathbf{x}_\alpha \in L_{sc}$. From now on, we impose the following condition.

ASSUMPTION 3.1 (Monotonicity condition in the z -direction). *The traveling time function u_0 , defined in (2.4) with \mathbf{n} replaced by \mathbf{n}_0 , is strictly increasing with respect to z . In other words,*

$$\partial_z u_0(\mathbf{x}, \mathbf{x}_\alpha) = \frac{\partial u_0(\mathbf{x}, \mathbf{x}_\alpha)}{\partial z} > 0$$

for all $\mathbf{x} = (x_1, \dots, x_{d-1}, z) \in \Omega$ and for all $\mathbf{x}_\alpha \in L_{sc}$.

Assumption 3.1 means that the higher in the z -direction, the longer the traveling time is. A sufficient condition for Assumption 3.1 to be true is formulated in (3.3) of Lemma 3.1. A similar monotonicity condition can be found in formulas (3.24) and (3.24') of section 2 of chapter 3 of the book [27]. Also, a similar condition was imposed in originating works for the 1D problem of Herglotz and Wiechert and

Zoeppritz [5, 35]: see section 3 of chapter 3 of [27]. Besides, figures 5 and 10 of [34] justify this condition from the geophysical standpoint. Although Lemma 3.1 is proven in [13] only in the 3D case, the proof in the d -D case is very similar and, therefore, avoided.

LEMMA 3.1 ([13]). *Let conditions (2.1) and (2.3) hold. Also, assume that $\mathbf{c}_0 \in C^2(\mathbb{R}^d)$, $\mathbf{c}_0 \geq m_0$ for some positive constant m_0 , $\mathbf{c}_0(\mathbf{x}) = 1$ for all $z < a$*

$$(3.3) \quad \partial_z c_0(\mathbf{x}) \geq 0 \quad \text{for all } \mathbf{x} \in \bar{\Omega}.$$

Then,

$$\partial_z u_0(\mathbf{x}, \mathbf{x}_\alpha) \geq \frac{a}{\sqrt{a^2 + 2}} \quad \text{for all } \mathbf{x} \in \bar{\Omega}, \alpha \in [-\bar{\alpha}, \bar{\alpha}].$$

Consider a new function $w(\mathbf{x}, \mathbf{x}_\alpha)$,

$$(3.4) \quad w(\mathbf{x}, \mathbf{x}_\alpha) = u(\mathbf{x}, \alpha) \partial_z u_0(\mathbf{x}, \mathbf{x}_\alpha) \quad \mathbf{x} \in \Omega, \mathbf{x}_\alpha \in L_{\text{sc}}.$$

We have

$$(3.5) \quad \begin{aligned} \partial_z u_0(\mathbf{x}, \mathbf{x}_\alpha) \partial_z u(\mathbf{x}, \mathbf{x}_\alpha) &= \partial_z w(\mathbf{x}, \mathbf{x}_\alpha) - u(\mathbf{x}, \alpha) \partial_{zz} u_0(\mathbf{x}, \mathbf{x}_\alpha) \\ &= \partial_z w(\mathbf{x}, \mathbf{x}_\alpha) - w(\mathbf{x}, \alpha) \frac{\partial_{zz} u_0(\mathbf{x}, \mathbf{x}_\alpha)}{\partial_z u_0(\mathbf{x}, \mathbf{x}_\alpha)}. \end{aligned}$$

and for $i = 1, \dots, d-1$

$$(3.6) \quad \begin{aligned} \partial_{x_i} u(\mathbf{x}, \mathbf{x}_\alpha) &= \frac{\partial}{\partial x_i} \left(\frac{w(\mathbf{x}, \mathbf{x}_\alpha)}{\partial_z u_0(\mathbf{x}, \mathbf{x}_\alpha)} \right) \\ &= \frac{\partial_{x_i} w(\mathbf{x}, \mathbf{x}_\alpha) \partial_z u_0(\mathbf{x}, \mathbf{x}_\alpha) - w(\mathbf{x}, \mathbf{x}_\alpha) \partial_{zx_i} u_0(\mathbf{x}, \mathbf{x}_\alpha)}{(\partial_z u_0(\mathbf{x}, \mathbf{x}_\alpha))^2} \end{aligned}$$

for all $\mathbf{x} \in \Omega, \mathbf{x}_\alpha \in L_{\text{sc}}$. Combining (3.2), (3.5) and (3.6), we obtain

$$(3.7) \quad \begin{aligned} \frac{\partial}{\partial \alpha} \left[\partial_z w(\mathbf{x}, \mathbf{x}_\alpha) - w(\mathbf{x}, \mathbf{x}_\alpha) \frac{\partial_{zz} u_0(\mathbf{x}, \mathbf{x}_\alpha)}{\partial_z u_0(\mathbf{x}, \mathbf{x}_\alpha)} \right. \\ \left. + \sum_{i=1}^{d-1} \frac{\partial_{x_i} w(\mathbf{x}, \mathbf{x}_\alpha) \partial_z u_0(\mathbf{x}, \mathbf{x}_\alpha) - w(\mathbf{x}, \mathbf{x}_\alpha) \partial_{zx_i} u_0(\mathbf{x}, \mathbf{x}_\alpha)}{(\partial_z u_0(\mathbf{x}, \mathbf{x}_\alpha))^2} \partial_{x_i} u_0(\mathbf{x}, \mathbf{x}_\alpha) \right] = 0. \end{aligned}$$

This is equivalent to

$$(3.8) \quad \begin{aligned} \partial_{\alpha z} w(\mathbf{x}, \mathbf{x}_\alpha) - \frac{\partial_{zz} u_0(\mathbf{x}, \mathbf{x}_\alpha)}{\partial_z u_0(\mathbf{x}, \mathbf{x}_\alpha)} \partial_\alpha w(\mathbf{x}, \mathbf{x}_\alpha) - \frac{\partial}{\partial \alpha} \left(\frac{\partial_{zz} u_0(\mathbf{x}, \mathbf{x}_\alpha)}{\partial_z u_0(\mathbf{x}, \mathbf{x}_\alpha)} \right) w(\mathbf{x}, \mathbf{x}_\alpha) \\ + \sum_{i=1}^{d-1} \left[\frac{\partial_{x_i} u_0(\mathbf{x}, \mathbf{x}_\alpha)}{\partial_z u_0(\mathbf{x}, \mathbf{x}_\alpha)} \partial_{\alpha x_i} w(\mathbf{x}, \mathbf{x}_\alpha) + \frac{\partial}{\partial \alpha} \left(\frac{\partial_{x_i} u_0(\mathbf{x}, \mathbf{x}_\alpha)}{\partial_z u_0(\mathbf{x}, \mathbf{x}_\alpha)} \right) \partial_{x_i} w(\mathbf{x}, \mathbf{x}_\alpha) \right. \\ \left. - \frac{\partial_{zx_i} u_0(\mathbf{x}, \mathbf{x}_\alpha) \partial_{x_i} u_0(\mathbf{x}, \mathbf{x}_\alpha)}{(\partial_z u_0(\mathbf{x}, \mathbf{x}_\alpha))^2} \partial_\alpha w(\mathbf{x}, \mathbf{x}_\alpha) \right. \\ \left. - \frac{\partial}{\partial \alpha} \left(\frac{\partial_{zx_i} u_0(\mathbf{x}, \mathbf{x}_\alpha) \partial_{x_i} u_0(\mathbf{x}, \mathbf{x}_\alpha)}{(\partial_z u_0(\mathbf{x}, \mathbf{x}_\alpha))^2} \right) w(\mathbf{x}, \mathbf{x}_\alpha) \right] = 0. \end{aligned}$$

We recall now the orthonormal basis $\{\Psi_n\}_{n=1}^\infty$ constructed at the beginning of this section. For each $\mathbf{x} \in \Omega$ and for all $\mathbf{x}_\alpha \in L_{sc}$, we write

$$(3.9) \quad w(\mathbf{x}, \mathbf{x}_\alpha) = \sum_{n=1}^{\infty} w_n(\mathbf{x}) \Psi_n(\alpha) \approx \sum_{n=1}^N w_n(\mathbf{x}) \Psi_n(\alpha),$$

$$(3.10) \quad w_n(\mathbf{x}) = \int_{-\bar{\alpha}}^{\bar{\alpha}} w(\mathbf{x}, \mathbf{x}_\alpha) \Psi_n(\alpha) d\alpha.$$

The ‘‘cut-off’’ number N is chosen numerically. We discuss the choice of N in more details in Section 5. Following our approximate mathematical model introduced in Section 1, we assume that the approximation \approx in (3.9) is an equality as well as

$$(3.11) \quad \partial_\alpha w(\mathbf{x}, \mathbf{x}_\alpha) = \sum_{n=1}^N w_n(\mathbf{x}) \Psi'_n(\alpha).$$

Plugging (3.9) and (3.11) into (3.8) gives

$$\begin{aligned} & \sum_{n=1}^N \partial_z w_n(\mathbf{x}) \Psi'_n(\alpha) - \frac{\partial_{zz} u_0(\mathbf{x}, \mathbf{x}_\alpha)}{\partial_z u_0(\mathbf{x}, \mathbf{x}_\alpha)} \sum_{n=1}^N w_n(\mathbf{x}) \Psi'_n(\alpha) \\ & - \frac{\partial}{\partial \alpha} \left(\frac{\partial_{zz} u_0(\mathbf{x}, \mathbf{x}_\alpha)}{\partial_z u_0(\mathbf{x}, \mathbf{x}_\alpha)} \right) \sum_{n=1}^N w_n(\mathbf{x}) \Psi_n(\alpha) + \sum_{i=1}^{d-1} \left[\frac{\partial_{x_i} u_0(\mathbf{x}, \mathbf{x}_\alpha)}{\partial_z u_0(\mathbf{x}, \mathbf{x}_\alpha)} \sum_{n=1}^N \partial_{x_i} w_n(\mathbf{x}) \Psi'_n(\alpha) \right. \\ & + \frac{\partial}{\partial \alpha} \left(\frac{\partial_{x_i} u_0(\mathbf{x}, \mathbf{x}_\alpha)}{\partial_z u_0(\mathbf{x}, \mathbf{x}_\alpha)} \right) \sum_{n=1}^N \partial_{x_i} w_n(\mathbf{x}) \Psi_n(\alpha) - \frac{\partial_{zx_i} u_0(\mathbf{x}, \mathbf{x}_\alpha) \partial_{x_i} u_0(\mathbf{x}, \mathbf{x}_\alpha)}{(\partial_z u_0(\mathbf{x}, \mathbf{x}_\alpha))^2} \sum_{n=1}^N w_n(\mathbf{x}) \Psi'_n(\alpha) \\ & \left. - \frac{\partial}{\partial \alpha} \left(\frac{\partial_{zx_i} u_0(\mathbf{x}, \mathbf{x}_\alpha) \partial_{x_i} u_0(\mathbf{x}, \mathbf{x}_\alpha)}{(\partial_z u_0(\mathbf{x}, \mathbf{x}_\alpha))^2} \right) \sum_{n=1}^N w_n(\mathbf{x}) \Psi_n(\alpha) \right] = 0. \end{aligned}$$

For each $m \in \{1, \dots, N\}$, multiply the latter equation by $\Psi_m(\alpha)$ and then integrate the resulting equation with respect to α . We get

$$(3.12) \quad \sum_{n=1}^N s_{mn} \partial_z w_n(\mathbf{x}) + \sum_{n=1}^N a_{mn}(\mathbf{x}) w_n(\mathbf{x}) + \sum_{n=1}^N \sum_{i=1}^{d-1} b_{mn,i}(\mathbf{x}) \partial_{x_i} w_n(\mathbf{x}) = 0$$

for all $\mathbf{x} \in \Omega$ where s_{mn} is defined as in Proposition 3.1,

$$(3.13) \quad a_{mn}(\mathbf{x}) = \int_{-\bar{\alpha}}^{\bar{\alpha}} \left[-\frac{\partial_{zz} u_0(\mathbf{x}, \mathbf{x}_\alpha)}{\partial_z u_0(\mathbf{x}, \mathbf{x}_\alpha)} \Psi'_n(\alpha) - \frac{\partial}{\partial \alpha} \left(\frac{\partial_{zz} u_0(\mathbf{x}, \mathbf{x}_\alpha)}{\partial_z u_0(\mathbf{x}, \mathbf{x}_\alpha)} \right) \Psi_n(\alpha) \right. \\ \left. - \sum_{i=1}^{d-1} \frac{\partial}{\partial \alpha} \left(\frac{\partial_{zx_i} u_0(\mathbf{x}, \mathbf{x}_\alpha) \partial_{x_i} u_0(\mathbf{x}, \mathbf{x}_\alpha)}{(\partial_z u_0(\mathbf{x}, \mathbf{x}_\alpha))^2} \right) \Psi'_n(\alpha) \right. \\ \left. - \sum_{i=1}^{d-1} \frac{\partial}{\partial \alpha} \left(\frac{\partial_{zx_i} u_0(\mathbf{x}, \mathbf{x}_\alpha) \partial_{x_i} u_0(\mathbf{x}, \mathbf{x}_\alpha)}{(\partial_z u_0(\mathbf{x}, \mathbf{x}_\alpha))^2} \right) \Psi_n(\alpha) \right] \Psi_m(\alpha) d\alpha$$

and for $i = 1, \dots, d-1$

$$(3.14) \quad b_{mn,i}(\mathbf{x}) = \int_{-\bar{\alpha}}^{\bar{\alpha}} \left[\frac{\partial_{x_i} u_0(\mathbf{x}, \mathbf{x}_\alpha)}{\partial_z u_0(\mathbf{x}, \mathbf{x}_\alpha)} \Psi'_n(\alpha) + \frac{\partial}{\partial \alpha} \left(\frac{\partial_{x_i} u_0(\mathbf{x}, \mathbf{x}_\alpha)}{\partial_z u_0(\mathbf{x}, \mathbf{x}_\alpha)} \right) \Psi_n(\alpha) \right] \Psi_m(\alpha) d\alpha,$$

for all $\mathbf{x} \in \Omega$. For each $\mathbf{x} \in \Omega$, let $W(\mathbf{x}) = (w_1(\mathbf{x}), \dots, w_N(\mathbf{x}))^T$, $S = (s_{mn})_{m,n=1}^N$, $A(\mathbf{x}) = (a_{mn}(\mathbf{x}))_{m,n=1}^N$ and $B_i(\mathbf{x}) = (b_{mn,i}(\mathbf{x}))_{m,n=1}^N$ for $i = 1, \dots, d-1$. Since (3.12) holds true for every $m = 1, \dots, N$, it can be rewritten as

$$(3.15) \quad S_N \partial_z W(\mathbf{x}) + A(\mathbf{x})W(\mathbf{x}) + \sum_{i=1}^{d-1} B_i(\mathbf{x}) \partial_{x_i} W(\mathbf{x}) = 0.$$

Since S is invertible, see Proposition 3.1, then (3.15) implies the following important system of transport equations

$$(3.16) \quad \partial_z W(\mathbf{x}) + S_N^{-1} A(\mathbf{x})W(\mathbf{x}) + \sum_{i=1}^{d-1} S_N^{-1} B_i(\mathbf{x}) \partial_{x_i} W(\mathbf{x}) = 0, \quad \mathbf{x} \in \Omega.$$

The boundary data for W are:

$$(3.17) \quad W|_{\partial\Omega} = F(\mathbf{x}) = (f_n)_{n=1}^N, \quad f_n(\mathbf{x}) = \int_{-\bar{\alpha}}^{\bar{\alpha}} f(\mathbf{x}, \mathbf{x}_\alpha) \partial_z u_0(\mathbf{x}, \mathbf{x}_\alpha) \Psi_n(\alpha) d\alpha$$

where f is the given data, see (2.6).

REMARK 3.2. *From now on, we consider the vector valued function $F(\mathbf{x})$ as the “indirect” data, which can be computed directly from (3.17). The noiseless data is denoted by F^* . The corresponding noisy data is*

$$(3.18) \quad F^\delta(\mathbf{x}) = F^*(1 + \delta \text{rand}(\mathbf{x})), \quad \mathbf{x} \in \partial\Omega$$

where $\delta > 0$ is the noise level and rand is a uniformly distributed function of random numbers taking the range in $[-1, 1]$.

REMARK 3.3 (The approximation context). *Due to the truncation in (3.9), equation (3.16) is within the framework of our approximate mathematical model mentioned in Introduction. Since this paper is concerned with computational rather than theoretical results, then this model is acceptable. Our approximation provides good numerical results in Section 5.*

REMARK 3.4. *Problem 2.1 is reduced to the problem of finding the vector valued function W satisfying the system (3.16) and the boundary condition (3.17). Assume this vector function is computed and denote it as $W^{\text{comp}} = (w_1^{\text{comp}}, \dots, w_n^{\text{comp}})$. Then, we can compute the function $w^{\text{comp}}(\mathbf{x}, \mathbf{x}_\alpha)$ and then the function $u^{\text{comp}}(\mathbf{x}, \mathbf{x}_\alpha)$ sequentially via (3.9) and (3.4). The computed target function $p^{\text{comp}}(\mathbf{x})$ is given by (2.10).*

We find an approximate solution of the boundary value problem (3.16)–(3.17) by the quasi-reversibility method. This means that we minimize the functional

$$(3.19) \quad J_\epsilon(W) = \int_{\Omega} \left| \partial_z W(\mathbf{x}) + \sum_{i=1}^{d-1} S_N^{-1} B_i(\mathbf{x}) \partial_{x_i} W(\mathbf{x}) + S_N^{-1} A(\mathbf{x})W(\mathbf{x}) \right|^2 d\mathbf{x} \\ + \epsilon \|W\|_{H^1(\Omega)^N}^2$$

on the set of vector functions $W \in H^1(\Omega)^N$ satisfying the boundary constraint (3.17). Here the space $H^1(\Omega)^N = \underbrace{H^1(\Omega) \times \dots \times H^1(\Omega)}_N$ with the commonly defined norm.

Similarly to [31], we analyze the functional $J_\epsilon(W)$ for the case when derivatives in (3.19) are written in finite differences.

The procedure of computing $p(\mathbf{x})$ is summarized in Algorithm 3.1.

Algorithm 3.1 The procedure to solve Problem 2.1

- 1: Choose the cut-off number $N = 35$, see Section 5 and Figure 1. Find $\{\Psi_n\}_{n=1}^N$.
- 2: Compute the boundary data of the vector valued function $W(\mathbf{x})$.
- 3: Minimize the functional $J_\epsilon(W)$ subjected to the boundary condition (3.17) to obtain $W^{\text{comp}}(\mathbf{x})$, $\mathbf{x} \in \Omega$.
- 4: Set $w^{\text{comp}}(\mathbf{x}, \mathbf{x}_\alpha) = \sum_{n=1}^N w_n^{\text{comp}} \Psi_n(\alpha)$, $\mathbf{x} \in \Omega$, $\alpha \in [-\bar{\alpha}, \bar{\alpha}]$.
- 5: Set $u^{\text{comp}} = w^{\text{comp}} / \partial_z u_0$. Compute p^{comp} by the average of the left hand side of (2.10), namely

$$(3.20) \quad p^{\text{comp}} = \frac{1}{2\bar{\alpha}} \int_{-\bar{\alpha}}^{\bar{\alpha}} \left[\partial_z u_0(\mathbf{x}, \mathbf{x}_\alpha) \partial_z u^{\text{comp}}(\mathbf{x}, \mathbf{x}_\alpha) + \sum_{i=1}^{d-1} \partial_{x_i} u_0(\mathbf{x}, \mathbf{x}_\alpha) \partial_{x_i} u^{\text{comp}}(\mathbf{x}, \mathbf{x}_\alpha) \right] d\alpha.$$

4. The quasi-reversibility method in the finite differences. For brevity, we describe and analyze here the quasi-reversibility method in the case when $d = 2$. The arguments for higher dimensions can be done in the same manner. In 2D, $\Omega = (-R, R) \times (a, b)$. We arrange an $N_x \times N_z$ grid of points on $\bar{\Omega}$

$$(4.1) \quad \mathcal{G} = \{(x_i, z_j) : x_i = -R + (i-1)h_x, z_j = a + (j-1)h_z, \\ i = 1, \dots, N_x, j = 1, \dots, N_z\},$$

where $h_x \in [h_0, \beta_x)$ and $h_z \in (0, \beta_z)$ are grid step sizes in the x and z directions respectively and $h_0, \beta_x, \beta_z > 0$ are certain numbers. Here, N_x and N_z are two positive integers. Let $\mathbf{h} = (h_x, h_z)$. We define the discrete set $\Omega^{\mathbf{h}}$ as the set of those points of the set (4.1) which are interior points of the rectangle Ω and $\partial\Omega^{\mathbf{h}}$ is the set of those points of the set (4.1) which are located on the boundary of Ω ,

$$\begin{aligned} \Omega^{\mathbf{h}} &= \{(x_i, z_j) : x_i = -R + (i-1)h_x, z_j = a + (j-1)h_z : \\ &\quad i = 2, \dots, N_x - 1; j = 2, \dots, N_z - 1\} \\ \partial\Omega^{\mathbf{h}} &= \{(\pm R, z_j) : j = 1, \dots, N_z\} \cup \{(x_i, z) : i = 1, \dots, N_x, z \in \{a, b\}\}, \\ \bar{\Omega}^{\mathbf{h}} &= \Omega^{\mathbf{h}} \cup \partial\Omega^{\mathbf{h}}. \end{aligned}$$

For any continuous function v defined on Ω its finite difference version is $v^{\mathbf{h}} = v|_{\mathcal{G}}$. Here, \mathbf{h} denotes the pair (h_x, h_z) . The partial derivatives of the function v are given via forward finite differences as

$$(4.2) \quad \begin{aligned} \partial_x^{h_x} v^{\mathbf{h}}(x_i, z_j) &= \frac{v^{\mathbf{h}}(x_{i+1}, z_j) - v^{\mathbf{h}}(x_i, z_j)}{h_x} \\ \partial_z^{h_z} v^{\mathbf{h}}(x_i, z_j) &= \frac{v^{\mathbf{h}}(x_i, z_{j+1}) - v^{\mathbf{h}}(x_i, z_j)}{h_z} \end{aligned}$$

for $i = 0, \dots, N_x - 1$ and $j = 0, \dots, N_z - 1$. We denote the finite difference analogs of the spaces $L^2(\Omega)$ and $H^1(\Omega)$ as $L^{2,\mathbf{h}}(\Omega)$ and $H^{1,\mathbf{h}}(\Omega)$. Norms in these spaces are

defined as

$$\begin{aligned} \|v^{\mathbf{h}}\|_{L^{2,\mathbf{h}}(\Omega^{\mathbf{h}})} &= \left[h_x h_z \sum_{i=0}^{N_x} \sum_{j=0}^{N_z} [v^{\mathbf{h}}(x_i, z_j)]^2 \right]^{1/2}, \\ \|v^{\mathbf{h}}\|_{H^{1,\mathbf{h}}(\Omega^{\mathbf{h}})} &= \left[\|v^{\mathbf{h}}\|_{L^{2,\mathbf{h}}(\Omega^{\mathbf{h}})}^2 + h_x h_z \sum_{i=0}^{N_x-1} \sum_{j=0}^{N_z-1} [\partial_x^{h_x} v^{\mathbf{h}}(x_i, z_j)]^2 \right. \\ &\quad \left. + [\partial_z^{h_z} v^{\mathbf{h}}(x_i, z_j)]^2 \right]^{1/2}. \end{aligned}$$

Let $F^{\mathbf{h}} = F|_{\partial\Omega^{\mathbf{h}}}$. The problem (3.16)–(3.17) becomes

$$(4.3) \quad L^{\mathbf{h}}(W^{\mathbf{h}}) = \partial_z^{h_z} W^{\mathbf{h}}(x_i, z_j) + S_N^{-1} B_1(\mathbf{x}_i, z_j) \partial_x^{h_x} W^{\mathbf{h}}(x_i, z_j) + S_N^{-1} A(x_i, z_j) W^{\mathbf{h}}(x_i, z_j) = 0$$

for $i = 0, \dots, N_x - 1; j = 0, \dots, N_z - 1$ and

$$(4.4) \quad W^{\mathbf{h}}|_{\partial\Omega^{\mathbf{h}}} = F^{\mathbf{h}}.$$

To solve problem (4.3)–(4.4) numerically, we introduce the finite difference version of the functional J_ϵ , defined in (3.19),

$$\begin{aligned} J_\epsilon^{\mathbf{h}}(W^{\mathbf{h}}) &= h_x h_z \sum_{i=0}^{N_x-1} \sum_{j=0}^{N_z-1} \left| \partial_z^{h_z} W^{\mathbf{h}}(x_i, z_j) + S_N^{-1} B_1(\mathbf{x}_i, z_j) \partial_x^{h_x} W^{\mathbf{h}}(x_i, z_j) \right. \\ &\quad \left. + S_N^{-1} A(x_i, z_j) W^{\mathbf{h}}(x_i, z_j) \right|^2 + \epsilon \|W^{\mathbf{h}}\|_{H_N^{1,\mathbf{h}}(\Omega^{\mathbf{h}})}^2, \end{aligned}$$

where $H_N^{1,\mathbf{h}}(\Omega^{\mathbf{h}}) = [H^{1,\mathbf{h}}(\Omega^{\mathbf{h}})]^N$ and similarly for $L_N^{2,\mathbf{h}}(\Omega^{\mathbf{h}})$. We consider the following problem:

PROBLEM 4.1 (Minimization Problem 1). *Minimize the functional $J_\epsilon^{\mathbf{h}}(W^{\mathbf{h}})$ on the set of such vector functions $W^{\mathbf{h}} \in H_N^{1,\mathbf{h}}(\Omega^{\mathbf{h}})$ that satisfy boundary condition (4.4).*

The convergence theory for this problem is formulated in Theorems 4.1 and 4.2. Proofs of these theorems follow closely the arguments of [31, Section 5] and are, therefore, not repeated in this paper. Theorem 4.1 guarantees the existence and uniqueness of the minimizer of $J_\epsilon^{\mathbf{h}}(W^{\mathbf{h}})$, and this result can be proven on the basis of Riesz theorem. The next natural and quite more complicated question is about the convergence of regularized solutions (i.e. minimizers) to the exact one when the level of the noise in the data tends to zero, i.e. Theorem 4.2. As it is quite often the case in the quasi-reversibility method (see, e.g. [10]), a close analog of Theorem 4.2 is proven in [31, Section 5] via applying a new discrete Carleman estimate: recall that conventional Carleman estimates are in the continuous form. In other words, these two theorems confirm the effectiveness of our proposed numerical method for solving Problem 2.1.

THEOREM 4.1 (existence and uniqueness of the minimizer). *For any $\mathbf{h} = (h_x, h_z)$ with $h_x \in [h_0, \beta_x)$, $h_z \in (0, \beta_z)$, any $\epsilon > 0$ and for any matrix $F^{\mathbf{h}}$ of boundary conditions there exists unique minimizer $W_{\min, \epsilon}^{\mathbf{h}} \in H_N^{1,\mathbf{h}}(\Omega^{\mathbf{h}})$ of the functional satisfying boundary condition (4.4).*

As it is always the case in the regularization theory, assume now that there exists an “ideal” solution $W_*^{\mathbf{h}} \in H_N^{1,\mathbf{h}}(\Omega^{\mathbf{h}})$ of problem (4.3)-(4.4) satisfying the following boundary condition:

$$(4.5) \quad W_*^{\mathbf{h}}|_{\partial\Omega^{\mathbf{h}}} = F_*^{\mathbf{h}},$$

where $F_*^{\mathbf{h}}$ is the “ideal” noiseless boundary data. Since $W_*^{\mathbf{h}}$ exists, (4.5) implies that there exists an extension $G_*^{\mathbf{h}} \in H_N^{1,\mathbf{h}}(\Omega^{\mathbf{h}})$ with $G_*^{\mathbf{h}}|_{\partial\Omega^{\mathbf{h}}} = F_*^{\mathbf{h}}$ of the matrix $F_*^{\mathbf{h}}$ in $\Omega^{\mathbf{h}}$. As to the data $F^{\mathbf{h}}$ in (4.4), we assume now that there exists an extension $G^{\mathbf{h}} \in H_N^{1,\mathbf{h}}(\Omega^{\mathbf{h}})$ with $G^{\mathbf{h}}|_{\partial\Omega^{\mathbf{h}}} = F^{\mathbf{h}}$ of $F^{\mathbf{h}}$ in $\Omega^{\mathbf{h}}$. Let $\delta > 0$ be the level of the noise in $G^{\mathbf{h}}$. We assume that

$$(4.6) \quad \|G^{\mathbf{h}} - G_*^{\mathbf{h}}\|_{H_N^{1,\mathbf{h}}(\Omega^{\mathbf{h}})} < \delta.$$

It is convenient to replace the above notation of the minimizer $W_{\min,\epsilon}^{\mathbf{h}}$ with $W_{\min,\epsilon,\delta}^{\mathbf{h}}$, thus, indicating its dependence on δ . In [31, Section 5], to prove a direct analog of Theorem 4.2 (formulated below), a new Carleman estimate for the finite difference operator $\partial_z^{h_z} v$ was proven first. The Carleman Weight Function of this estimate depends only on the discrete variable z . The value of this function at the point $z_j = a + (j-1)h_z$ is $e^{2\lambda(j-1)h_z}$, where $\lambda > 0$ is a parameter. This estimate is valid only if $\lambda h_z < 1$ (Lemma 4.7 of [31, Section 5]). The latter explains the condition of Theorem 4.2 imposed on the grid step size h_z in the z -direction.

THEOREM 4.2 (convergence of regularized solutions). *Let conditions (4.5) and (4.6) be valid. Let $L^{\mathbf{h}}$ be the operator in (4.3). Let $W_{\min,\epsilon,\delta}^{\mathbf{h}} \in H_N^{1,\mathbf{h}}(\Omega^{\mathbf{h}})$ be the minimizer of the functional $J_{\epsilon}^{\mathbf{h}}(W^{\mathbf{h}})$ with boundary condition (4.4). Then there exists a sufficiently small number $\bar{h}_z > 0$ depending only on $h_0, a, b, R, N, L^{\mathbf{h}}$ such that the following estimate is valid for all $(h_x, h_z) \in [h_0, \beta_x) \times (0, \bar{h}_z)$ and all $\epsilon, \delta > 0$ with a constant $C > 0$ independent on ϵ, δ*

$$\|W_{\min,\epsilon,\delta}^{\mathbf{h}} - W_*^{\mathbf{h}}\|_{L_N^{2,\mathbf{h}}(\Omega^{\mathbf{h}})} \leq C \left(\delta + \sqrt{\epsilon} \|W_*^{\mathbf{h}}\|_{H_N^{1,\mathbf{h}}(\Omega^{\mathbf{h}})} \right).$$

We also note that Lipschitz stability estimate for problem (4.3)-(4.4) is valid as a direct analog of Theorem 5.5 of [31, Section 5]. Therefore, uniqueness also takes place for problem (4.3)-(4.4).

5. Numerical Implementation. In this section, we solve Problem 2.1 in the 2D case. The domain Ω is

$$(5.1) \quad \Omega = (-1, 1) \times (1, 3).$$

The line of sources L_{sc} is set to be $(-\bar{\alpha}, \bar{\alpha})$ with $\bar{\alpha} = 3$.

We solve the forward problem to compute the simulated data as follows. Given the background function \mathbf{n}_0 , instead of solving the nonlinear Eikonal equation (2.9), we find $u_0(\mathbf{x}, \mathbf{x}_\alpha)$ using (2.4). The geodesic line $\Gamma(\mathbf{x}, \mathbf{x}_\alpha)$ connecting $\mathbf{x} \in \Omega$ and $\mathbf{x}_\alpha \in L_{sc}$ in (2.4) can be found by using the 2D Fast Marching toolbox which is built in Matlab. The Fast Marching is very similar to the Dijkstra algorithm to find the shortest paths on graphs. We refer the reader to [30] for more details about Fast Marching. Next, with this geodesic line in hand, we compute

$$u(\mathbf{x}, \mathbf{x}_\alpha) = \int_{\Gamma(\mathbf{x}, \mathbf{x}_\alpha)} p(\mathbf{x}) d\sigma(\mathbf{x}).$$

It is clear that the function u solves (2.5). The point \mathbf{x}_α above is chosen as $(\alpha_i, 0)$ where $\alpha_i = 2(i-1)\bar{\alpha}/N_\alpha$. In this paper, we set $N_\alpha = 209$.

We now explain how do we find an appropriate cut-off number N in (3.9). We take the data $f(\mathbf{x}, \mathbf{x}_\alpha)$ in Test 5 in subsection 5.2. Then, we compare the function $w(x, z = b, \mathbf{x}_\alpha)$ and its approximation $\sum_{n=1}^N f_n(x, z = b)\Psi_n(\alpha)$ where f_n is defined in (3.17). The first row in Figure 1 shows the graphs of

$$e_N(x, \alpha) = \left| w(x, z = b, \mathbf{x}_\alpha) - \sum_{n=1}^N f_n(x, z = b, \mathbf{x}_\alpha) \right|, \quad x \in (-R, R), \alpha \in (-\bar{\alpha}, \bar{\alpha})$$

when $N = 10, 15$ and 35 . The second row in Figure 1 shows the true function w and its approximation at $z = b$ and $\alpha = 1.28$. It is obvious that the sum in the right hand side of the first equation in (3.9) when $N = 35$ is a good approximation of the data. Thus, we select $N = 35$ in this paper.

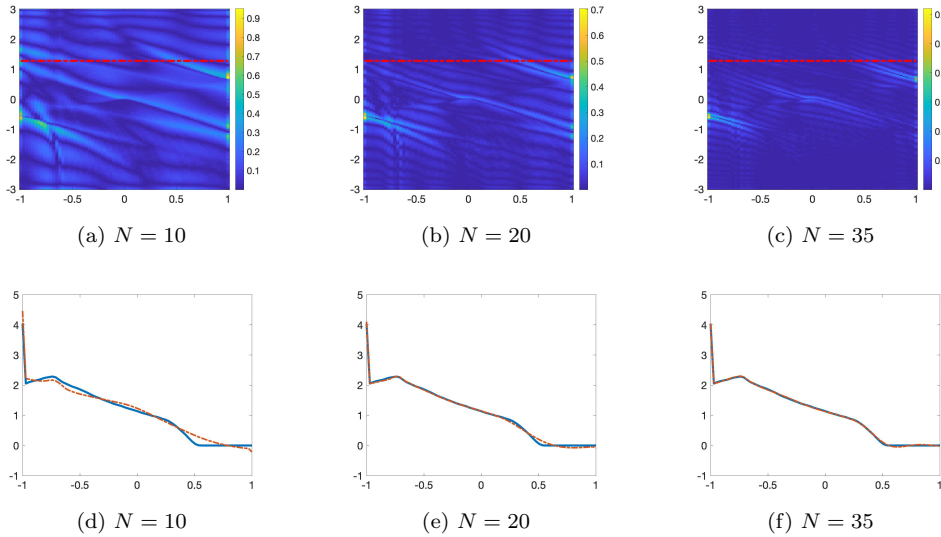


Figure 1: The graphs of the functions $e_N(x, \alpha)$ for $N = 10, 20$ and 35 . The first row shows the 2D graph of e_N and the second row shows the function $w_{\text{true}}(x, z = b, \alpha = 1.28)$ and the function $\sum_{n=1}^N w_n(x, z = b)\Psi_n(\alpha = 1.28)$. We observe that the larger N , the smaller difference of the data and its approximation is.

5.1. Computing W^{comp} . We arrange the grid \mathcal{G} in $\bar{\Omega}$ as in (4.1). For simplicity, we choose $N_{\mathbf{x}} = N_x = N_z$. The step size $h = h_x = h_z = 2R/(N_{\mathbf{x}} - 1)$. We observe numerically that the matrix S_N^{-1} , present in the definition of J_ϵ in (3.19), contains some large numbers. This causes some unwanted errors in computations. Therefore, we slightly modify the functional J_ϵ , see in (3.19), suggested by (3.16), by the following

functional (due to (3.15))

$$(5.2) \quad I_\epsilon(W) = \int_{\Omega} |S_N \partial_z W(\mathbf{x}) + A(\mathbf{x})W(\mathbf{x}) + \sum_{i=1}^{d-1} B_i(\mathbf{x}) \partial_{x_i} W(\mathbf{x})|^2 d\mathbf{x} \\ + \epsilon \|W\|_{H^1(\Omega)^N}^2 + \epsilon \|\Delta W\|_{L^2(\Omega)^N}^2.$$

We have numerically observed that the additional regularization term $\epsilon \|\Delta W\|_{L^2(\Omega)^N}^2$ in (5.2) is crucial. Without it, the numerical results do not meet our expectation. In all tests with all noise level in the data, we choose $\epsilon = 10^{-7}$ by a trial and error process. The finite difference version of the functional I_ϵ for $d = 2$ is

$$I_\epsilon^h(W) = h^2 \sum_{m=1}^N \sum_{i,j=1}^{N_x-1} \left| \sum_{n=1}^N \left[\frac{s_{mn}[w_n(x_i, z_{j+1}) - w_n(x_i, z_j)]}{h} \right. \right. \\ \left. \left. + a_{mn}(x_i, z_j)w(x_i, y_j) + \frac{b_{mn}(x_i, z_j)(w(x_{i+1}, z_j) - w(x_i, z_j))}{h} \right] \right|^2 \\ + \epsilon h^2 \sum_{n=1}^N \sum_{i,j=0}^{N_x} |w_n(x_i, z_j)|^2 + \epsilon h^2 \sum_{n=1}^N \sum_{i,j=0}^{N_x-1} [|\partial_x^h w_n(x_i, z_j)|^2 + |\partial_z^h w_n(x_i, z_j)|^2] \\ + \epsilon h^2 \sum_{n=1}^N \sum_{i,j=1}^{N_x-1} |\partial_{xx} w_n(x_i, z_j)|^2 + \epsilon h^2 \sum_{n=1}^N \sum_{i,j=1}^{N_x-1} |\partial_{zz} w_n(x_i, z_j)|^2$$

where a_{mn} and $b_{mn} = b_{mn,1}$ in (3.13) and (3.14) respectively. The partial derivatives ∂_x^h and ∂_z^h are as in (4.2). The second derivatives in finite difference are understood as usual. We next line up the discrete vector valued function $w_n(x_i, z_j)$, $1 \leq i, j \leq N_x$, $1 \leq n \leq N$ as the vector $(\mathbf{w}_i)_{i=1}^{N_x^2 N}$ with

$$(5.3) \quad \mathbf{w}_i = w_n(x_i, z_j)$$

where

$$(5.4) \quad \mathbf{i} = (i-1)N_x N + (j-1)N + n.$$

The functional I_ϵ^h in the ‘‘line up’’ version is

$$(5.5) \quad I_\epsilon^h(\mathbf{w}) = h^2 \left[|\mathcal{L}\mathbf{w}|^2 + \epsilon |D_x \mathbf{w}|^2 + \epsilon |D_y \mathbf{w}|^2 + \epsilon |L\mathbf{w}|^2 \right].$$

In (5.5),

1. \mathcal{L} is the $N_x^2 N \times N_x^2 N$ matrix with entries given by
 - (a) $(\mathcal{L})_{ij} = -s_{mn}/h + a_{mn}(x_i, z_j) - b_{mn}(x_i, y_j)/h$ for $\mathbf{i} = (i-1)N_x N + (j-1)N + m$ and $\mathbf{j} = (i-1)N_x N + (j-1)N + n$,
 - (b) $(\mathcal{L})_{ij} = b_{mn}(x_i, z_j)/h$ for $\mathbf{i} = (i-1)N_x N + (j-1)N + m$ and $\mathbf{j} = (i+1-1)N_x N + (j-1)N + n$,
 - (c) $(\mathcal{L})_{ij} = s_{mn}/h$ for $\mathbf{i} = (i-1)N_x N + (j-1)N + m$ and $\mathbf{j} = (i-1)N_x N + (j+1-1)N + n$,
 - (d) the other entries of \mathcal{L} are 0
 for $1 \leq i, j \leq N_x - 1$ and $1 \leq m, n \leq N$;
2. D_x is the $N_x^2 N \times N_x^2 N$ matrix with entries given by

- (a) $(D_x)_{ii} = -1/h$ for $\mathbf{i} = (i-1)N_xN + (j-1)N + m$,
 - (b) $(D_x)_{ij} = 1/h$ for $\mathbf{i} = (i-1)N_xN + (j-1)N + m$ and $\mathbf{j} = (i+1-1)N_xN + (j-1)N + m$,
 - (c) the other entries of \mathcal{L} are 0
- for $1 \leq i, j \leq N_x - 1$ and $1 \leq m \leq N$;
3. D_y is the $N_x^2N \times N_x^2N$ matrix with entries given by
- (a) $(D_y)_{ii} = -1/h$ for $\mathbf{i} = (i-1)N_xN + (j-1)N + m$,
 - (b) $(D_y)_{ij} = 1/h$ for $\mathbf{i} = (i-1)N_xN + (j-1)N + m$ and $\mathbf{j} = (i-1)N_xN + (j+1-1)N + m$,
 - (c) the other entries of \mathcal{L} are 0
- for $1 \leq i, j \leq N_x - 1$ and $1 \leq m \leq N$;
4. L is the $N_x^2N \times N_x^2N$ matrix with entries given by
- (a) $(L)_{ii} = -4/h^2$ for $\mathbf{i} = (i-1)N_xN + (j-1)N + m$,
 - (b) $(L)_{ij} = -1/h^2$ for $\mathbf{i} = (i-1)N_xN + (j-1)N + m$ and $\mathbf{j} = (i \pm 1 - 1)N_xN + (j-1)N + m$,
 - (c) $(L)_{ij} = -1/h^2$ for $\mathbf{i} = (i-1)N_xN + (j-1)N + m$ and $\mathbf{j} = (i-1)N_xN + (j \pm 1 - 1)N + m$,
 - (d) the other entries of \mathcal{L} are 0
- for $2 \leq i, j \leq N_x - 1$ and $1 \leq m \leq N$.
- The minimizer \mathbf{w} of I_ϵ^h satisfies the equation

$$(5.6) \quad \mathcal{L}^T \mathcal{L} + \epsilon(\text{Id} + D_x^T D_x + D_y^T D_y + L^T L) \mathbf{w} = 0.$$

On the other hand, due to the constraint (3.17)

$$(5.7) \quad \mathcal{D} \mathbf{w} = \mathbf{f}$$

where \mathcal{D} is a $N_x^2N \times N_x^2N$ matrix and \mathbf{f} is a N_x^2N dimensional vector, both of which are defined below

1. $(\mathcal{D})_{ii} = 1$ for $\mathbf{i} = (i-1)N_xN + (j-1)N + m$;
2. $(\mathbf{f})_{\mathbf{i}} = f_m(x_i, y_j)$ for $\mathbf{i} = (i-1)N_xN + (j-1)N + m$;
3. the other entries of \mathcal{L} and \mathbf{f} are 0

for $i \in \{1, N_x\}$, $1 \leq j \leq N_x$ or $2 \leq i \leq N_x - 1$, $j \in \{1, N_x\}$ and $1 \leq m \leq N$. Here, $(f_m)_{m=1}^N$ is in (3.17). Since the data might be noisy, see (3.18), we slightly modify the system constituted by (5.6) and (5.7) to a more stable version

$$(5.8) \quad \left(\begin{bmatrix} \mathcal{L} \\ \mathcal{D} \end{bmatrix}^T \begin{bmatrix} \mathcal{L} \\ \mathcal{D} \end{bmatrix} + \epsilon(\text{Id} + D_x^T D_x + D_y^T D_y + L^T L) \right) \mathbf{w} = \begin{bmatrix} 0 \\ \mathbf{f} \end{bmatrix}.$$

Solving the system (5.8), we obtain \mathbf{w}^{comp} . The values of components of vector valued function $W^{\text{comp}}(\mathbf{x})$ at grid points are computed as $w_n(x_i, z_j) = \mathbf{w}_{\mathbf{i}}$ for $\mathbf{i} = (i-1)N_xN + (j-1)N + m$, $1 \leq i, j \leq N_x$, $1 \leq m \leq N$, see (5.3).

We have presented the implementation of Step 3 in Algorithm 3.1. The other steps are straight forward.

REMARK 5.1 (Postprocessing). *In Step 5 of Algorithm 3.1 when computing p^{comp} using (3.20), which involves ∇u^{comp} , we smooth out u^{comp} by replacing the value of $u^{\text{comp}}(x, y, \alpha)$ $\alpha \in [-\bar{\alpha}, \bar{\alpha}]$ by the average of u^{comp} on the rectangle of 5×5 points around the point (x, y) . We also apply the same smoothing technique for the function p^{comp} .*

5.2. Numerical Tests. We perform four (4) numerical tests in this paper. When indicating dependence of any function below on x, z , we assume that $(x, z) \in \Omega$, where the domain Ω is defined in (5.1).

REMARK 5.2 (The function c_0). *In all our tests below, the function c_0 is far away from the constant background function. Therefore, Problem 2.1 is not considered as a small perturbation of the problem of inverse Radon transform with incomplete data, see [15]. All functions c_0 in our tests might not smooth in \mathbb{R}^2 but $c_0 \in C^1(\bar{\Omega})$ in Tests 2,3. Thus, the second derivatives of the corresponding function u_0 are well-defined in these two tests. Even though $c_0 \notin C^1(\bar{\Omega})$ in Test 1, numerically we have not experienced problems with second derivatives of the function u_0 .*

Test 1. The true source function p is given by

$$p^{\text{true}}(x, z) = \begin{cases} 8 & (x - 0.5)^2 + (z - 2)^2 < 0.22^2, \\ 5 & (x + 0.5)^2 + (z - 2)^2 < 0.2^2, \\ 0 & \text{otherwise.} \end{cases}$$

The background function c_0 is

$$c_0(x, z) = \begin{cases} 1 + 0.3(1 - x^2)(z^2 - 2) & \text{if } z^2 - 2 > 0, \\ 1 & \text{otherwise.} \end{cases}$$

The numerical results of this test are displayed in Figure 2.

The support of p^{true} in Test 1 consists of two discs. The value of the function p in the right disc is higher than the value in the left disc. Our method detects both these inclusions very well, see Figures 2c–2f. There are some unwanted artifacts near $\partial\Omega$ where we measure the noisy data. The higher level of noisy data, the more artifacts present. When the noise level $\delta = 5\%$, the computed maximal value of p^{comp} in the left inclusion is 5.16 (relative error 3.2%) and the computed maximal value of p^{comp} in the right inclusion is 7.72 (relative error 3.5%). When the noise level $\delta = 120\%$, the computed maximal value of p^{comp} in the left inclusion is 4.71 (relative error 5.8%) and the computed maximal value of p^{comp} in the right inclusion is 9.37 (relative error 17.1%).

Test 2. We test a complicated case when the support of p_{true} looks like a ring. In this test,

$$p^{\text{true}}(x, z) = \begin{cases} 2 & 0.55^2 < r^2 = x^2 + (z - 2)^2 < 0.75^2, \\ 0 & \text{otherwise.} \end{cases}$$

The background function c_0 is given by

$$c_0(x, z) = \begin{cases} 1 + 0.25(x - 0.5)^2 \ln(z) & z > 1, \\ 1 & \text{otherwise.} \end{cases}$$

The numerical results of this test are displayed in Figure 3.

In this test, it is evident that the reconstructed “ring” is acceptable, see Figures 3c and 3e. The position of the ring is detected quite well, see Figures 3d and 3f. When the noise level is 5%, the reconstructed maximal value of p^{comp} in the ring is 2.23 (relative error 11.5%). When the noise level is 30%, the reconstructed maximal value of p^{comp} in the ring is 2.42 (relative error 21.0%).

Test 3. We test an interesting and complicated case of the up-side-down letter Y

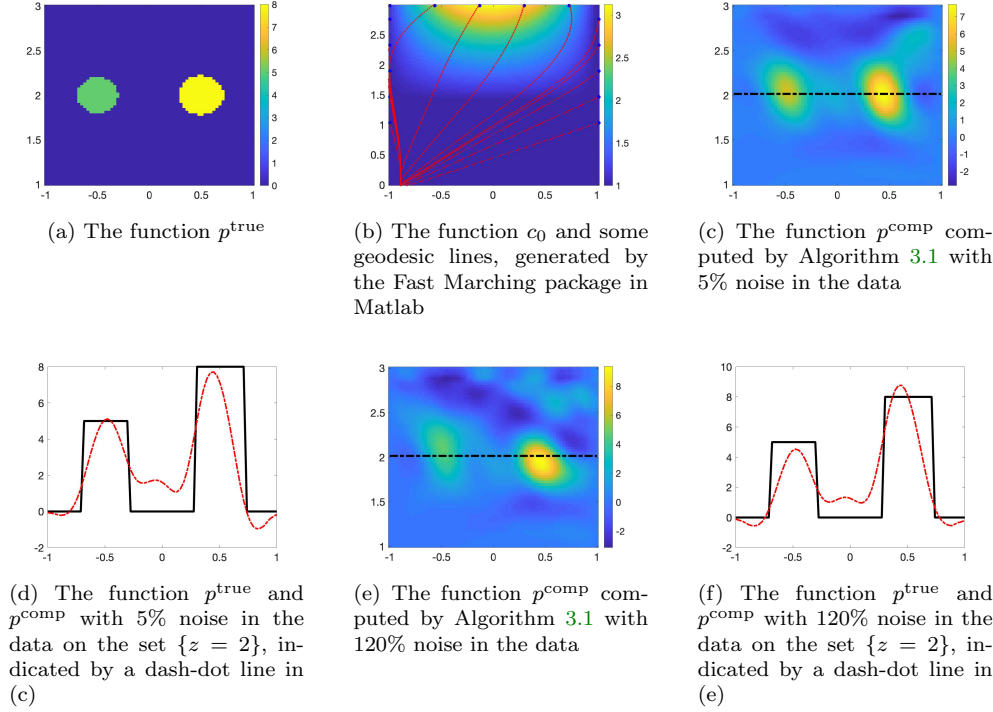


Figure 2: Test 1. The true and reconstructed source functions using Algorithm 3.1 from noisy data.

having both positive and negative values. In this test, the function p_{true} is given by

$$p^{\text{true}}(x, z) = \begin{cases} 2.5 & |x - (z - 2)| < 0.35, \max\{|x|, |z - 2|\} < 0.7, z < 2, x < 0, \\ -2.5 & |x + (z - 2)| < 0.2, \max\{|x|, |z - 2|\} < 0.7, z < 2, x > 0, \\ 2.5 & |x| < 0.2, \max\{|x|, |z - 2|\} < 0.8, z > 2, x < 0, \\ -2.5 & |x| < 0.2, \max\{|x|, |z - 2|\} < 0.8, z > 2, x > 0. \end{cases}$$

The background function c_0 is given by

$$c_0(x, z) = \begin{cases} 1 + 0.5(x + 0.5)^2 \ln(z) & z > 1, \\ 1 & \text{otherwise.} \end{cases}$$

The numerical results of this test are displayed in Figure 4.

It is clear from Figure 4 that both positive and negative parts of the function $p(x, z)$ are successfully identified. When the noise level $\delta = 5\%$, the reconstructed maximal value of the positive part of p^{comp} is 2.25 (relative error 10.0%) and the reconstructed minimal value of p^{comp} of the negative part is -2.74 (relative error 9.6%.) When the noise level is $\delta = 80\%$, the reconstructed maximal value of p^{comp} of the positive part is 2.30 (relative error 8.0%) and the reconstructed minimal value of p^{comp} of the negative part is -2.82 (relative error 12.8%.)

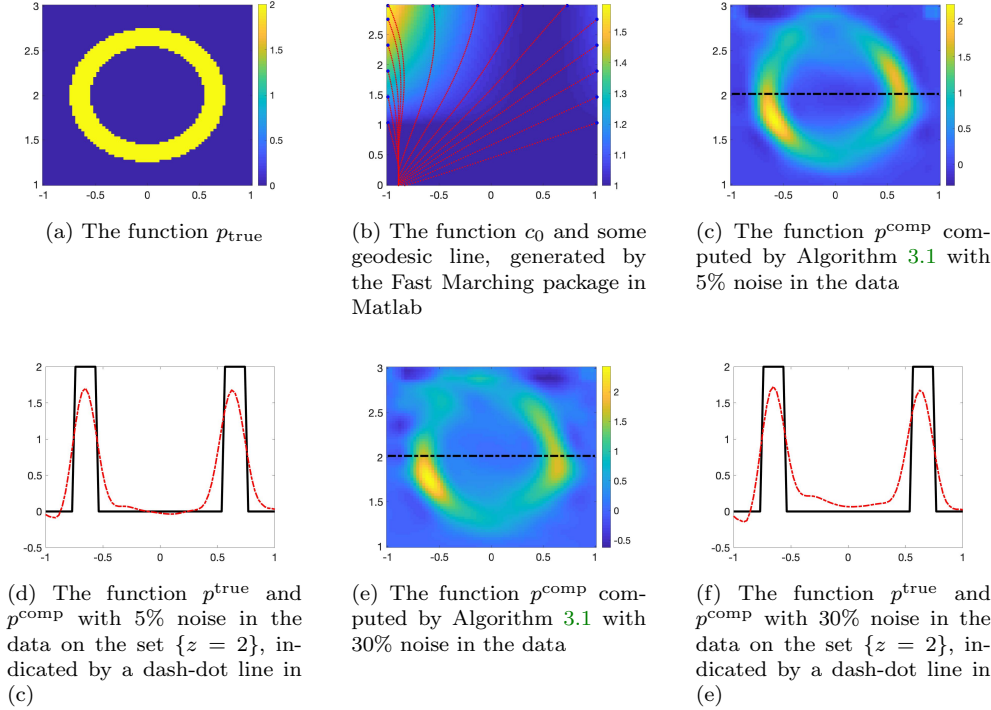


Figure 3: Test 2. The true and reconstructed source functions using Algorithm 3.1 from noisy data.

Test 4. In this test, we reconstruct the letter λ . The function p^{true} is given by

$$p^{\text{true}}(x, z) = \begin{cases} 2 & |x - (z - 2)| < 0.325, \max\{|x|, |z - 2|\} < 0.7 \text{ and } x < -0.03, \\ 2 & |x + (z - 2)| < 0.2 \text{ and } \max\{|x|, |z - 2|\} < 0.7, \\ 0 & \text{otherwise.} \end{cases}$$

In this test, we chose c_0 as

$$c_0(x, z) = \begin{cases} 1 + x^2 \ln(z) & z > 1, \\ 1 & \text{otherwise.} \end{cases}$$

The numerical results of this test are displayed in Figure 5.

The letter λ and the values of the function p^{true} are successfully reconstructed. The computed position of λ is a quite accurate one, see Figures 5d and 5f. When the noise level $\delta = 5\%$, the computed maximal value of p^{comp} is 2.31 (relative error 15.5%). When the noise level $\delta = 100\%$, the computed maximal value of p^{comp} is 3.27 (relative error 63.5%).

6. Concluding Remarks. In this paper, we have developed a convergent numerical method of the solution of the linearized Travel Time Tomography Problem with non-redundant incomplete data. A good accuracy of numerical results with 5% noise in the data is demonstrated for rather complicated functions to be imaged. It is quite surprising that an acceptable accuracy of computational results is observed

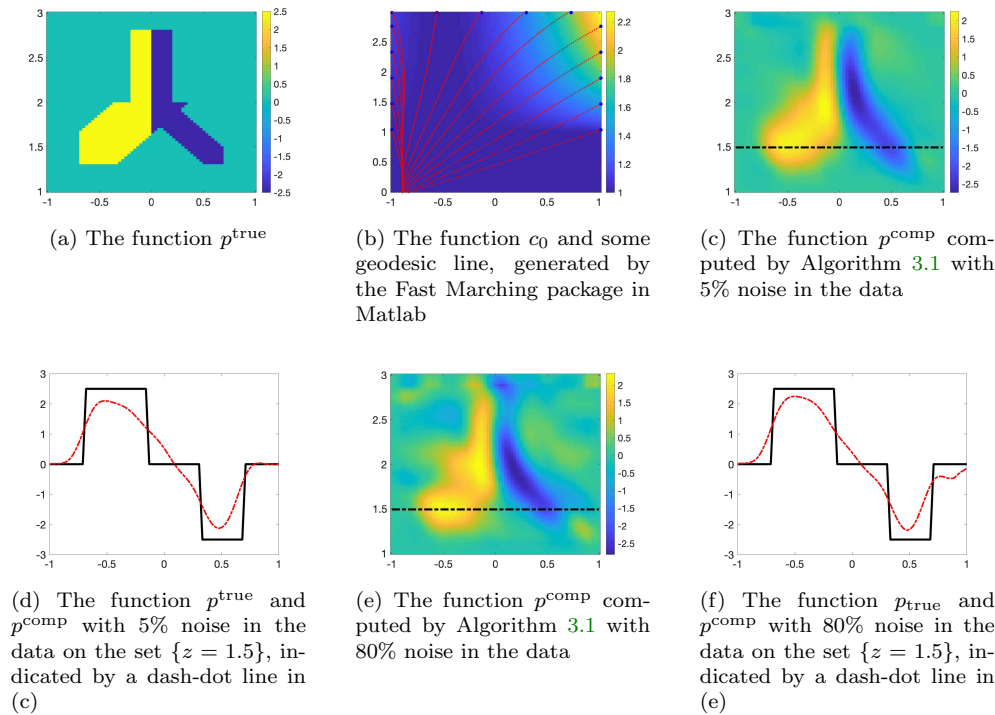


Figure 4: Test 3. The true and reconstructed source functions using Algorithm 3.1 from noisy data.

even for very high level of noise in the data varying between 30% and 120%.

REFERENCES

- [1] I. N. BERNSTEIN AND M. L. GERVER, *On a problem of integral geometry for family of geodesics and the inverse kinematic problem of seismic*, Dokl. Akad. Nauk SSSR, 243 (1978).
- [2] L. BOURGEOIS AND J. DARDÉ, *A duality-based method of quasi-reversibility to solve the Cauchy problem in the presence of noisy data*, Inverse Problems, 26 (2010), p. 095016.
- [3] L. BOURGEOIS, D. PONOMAREV, AND J. DARDÉ, *An inverse obstacle problem for the wave equation in a finite time domain*, Inverse Probl. Imaging, 13 (2019), pp. 377–400.
- [4] J. GUILLEMENT AND R. G. NOVIKOV, *Inversion of weighted Radon transforms via finite Fourier series weight approximation*, Inverse Problems in Science and Engineering, 22 (2013), pp. 787–802.
- [5] G. HERGLOTZ, *Aeber die Elastizitaet der Erde bei Beruecksichtigung ihrer variablen Dichte*, Zeitschr. fur Math. Phys., 52 (1905), pp. 275–299.
- [6] V. ISAKOV, *Inverse Problems for Partial Differential Equations*, Springer, New York, third ed., 2017.
- [7] S. I. KABANIKHIN, *Projection-Difference Methods for Determining of Hyperbolic Equations Coefficients*, Nauka, Novosibirsk, 1988.
- [8] S. I. KABANIKHIN, K. K. SABELFELD, N. S. NOVIKOV, AND M. A. SHISHLENIN, *Numerical solution of the multidimensional Gelfand-Levitan equation*, J. Inverse and Ill-Posed Problems, 23 (2015), pp. 439–450.
- [9] S. I. KABANIKHIN, A. D. SATYBAEV, AND M. A. SHISHLENIN, *Direct Methods of Solving Inverse Hyperbolic Problems*, VSP, Utrecht, 2005.
- [10] M. V. KLIBANOV, *Carleman estimates for the regularization of ill-posed Cauchy problems*,

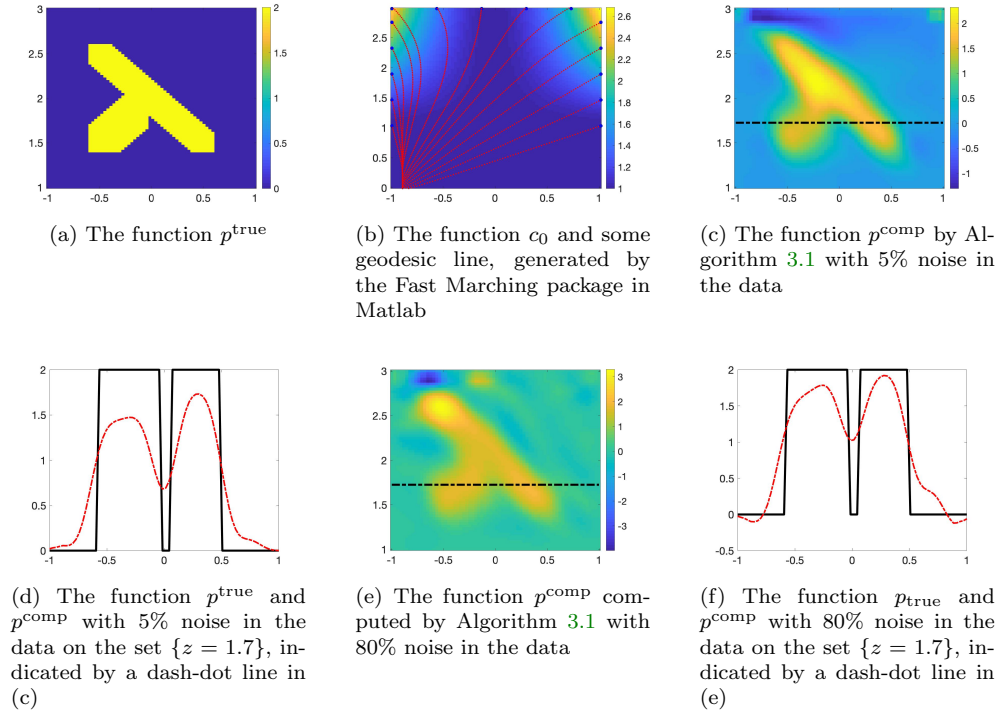


Figure 5: Test 4. The true and reconstructed source functions using Algorithm 3.1 from noisy data.

Applied Numerical Mathematics, 94 (2015), pp. 46–74.

[11] M. V. KLIBANOV, *Convexification of restricted Dirichlet to Neumann map*, J. Inverse and Ill-Posed Problems, 25 (2017), pp. 669–685.

[12] M. V. KLIBANOV, *On the travel time tomography problem in 3D*, Journal of Inverse and Ill-posed Problems, 27 (2019), pp. 591–607.

[13] M. V. KLIBANOV, *Travel time tomography with formally determined incomplete data in 3D*, Inverse Problems and Imaging, 13 (2019), pp. 1367–1393.

[14] M. V. KLIBANOV, J. LI, AND W. ZHANG, *Convexification for the inversion of a time dependent wave front in a heterogeneous medium*, Inverse Problems, 35 (2019), p. 035005.

[15] M. V. KLIBANOV AND L. H. NGUYEN, *PDE-based numerical method for a limited angle X-ray tomography*, Inverse Problems, 35 (2019), p. 045009.

[16] M. V. KLIBANOV, L. H. NGUYEN, AND K. PAN, *Nanostructures imaging via numerical solution of a 3-d inverse scattering problem without the phase information*, Appl. Numer. Math., 110 (2016), pp. 190–203.

[17] M. V. KLIBANOV AND V. G. ROMANOV, *Reconstruction procedures for two inverse scattering problems without the phase information*, SIAM J. Applied Mathematics, 76 (2016), pp. 178–196.

[18] R. LATTÈS AND J. L. LIONS, *The Method of Quasireversibility: Applications to Partial Differential Equations*, Elsevier, New York, 1969.

[19] T. T. LE AND L. H. NGUYEN, *A convergent numerical method to recover the initial condition of nonlinear parabolic equations from lateral Cauchy data*, preprint, arXiv:1910.05584, (2019).

[20] Q. LI AND L. H. NGUYEN, *Recovering the initial condition of parabolic equations from lateral Cauchy data via the quasi-reversibility method*, Inverse Problems in Science and Engineering, DOI: 10.1080/17415977.2019.1643850, (2019).

[21] F. MONARD, *Numerical implementation of geodesic X-ray transforms and their inversion*, SIAM J. Imaging Sci., 7 (2014), pp. 1335–1357.

- [22] R. G. MUKHOMETOV, *The reconstruction problem of a two-dimensional Riemannian metric and integral geometry*, Soviet Math. Dokl., 18 (1977), pp. 32–35.
- [23] R. G. MUKHOMETOV AND V. G. ROMANOV, *On the problem of determining an isotropic Riemannian metric in the n -dimensional space*, Dokl. Acad. Sci. USSR, 19 (1978), pp. 1330–1333.
- [24] L. H. NGUYEN, Q. LI, AND M. V. KLIBANOV, *A convergent numerical method for a multi-frequency inverse source problem in inhomogenous media*, Inverse Problems and Imaging, 13 (2019), pp. 1067–1094.
- [25] L. PESTOV AND G. UHLMANN, *Two dimensional simple Riemannian manifolds are boundary distance rigid*, Annals of Mathematics, 161 (2005), pp. 1093–1110.
- [26] V. G. ROMANOV, *Integral geometry on isotropic riemannian metric*, Dokl. Akad. Nauk SSSR, 241 (1978), pp. 290–293.
- [27] V. G. ROMANOV, *Inverse Problems of Mathematical Physics Physics*, VNU Press, Utrecht, 1986.
- [28] V. G. ROMANOV, *Problem of determining the permittivity in the stationary system of Maxwell equations*, Doklady Mathematics, 93 (2017), pp. 1–5.
- [29] U. SCHRÖDER AND T. SCHUSTER, *An iterative method to reconstruct the refractive index of a medium from time-off-light measurements*, Inverse Problems, 32 (2016), p. 085009.
- [30] J. A. SETHIAN, *Level Set Methods and Fast Marching Methods: Evolving Interfaces in Computational Geometry, Fluid Mechanics, Computer Vision, and Materials Science*, Cambridge Monograph on Applied and Computational Mathematics, Cambridge University Press, 1999.
- [31] A. V. SMIRNOV, M. V. KLIBANOV, AND L. H. NGUYEN, *On an inverse source problem for the full radiative transfer equation with incomplete data*, SIAM Journal on Scientific Computing., 41 (2019), pp. B929–B952.
- [32] P. STEFANOV, G. UHLMANN, AND A. VASY, *Local and global boundary rigidity and the geodesic X-ray transform in the normal gauge*, preprint arXiv: 1702.03638v2, 2017, (2017).
- [33] P. STEFANOV, G. UHLMANN, AND A. VASY, *Inverting the local geodesic X-ray transform on tensors*, Journal d’Analyse Mathématique, 136 (2018), pp. 151–208.
- [34] L. VOLGYESI AND M. MOSER, *The inner structure of the Earth*, Periodica Polytechnica Chemical Engineering, 26 (1982), pp. 155–204.
- [35] E. WIECHERT AND J. ZOEPFPRITZ, *Über Erdbebenwellen*, Nachr. Koenigl. Gesellschaft Wiss. Gottingen, 4 (1907), pp. 415–549.
- [36] H. ZHAO AND Y. ZHONG, *A hybrid adaptive phase space method for reflection travel time tomography*, SIAM J. Imaging Sci., 12 (2019), pp. 28–53.